Available online at www.sciencedirect.com
ScienceDirect
Trans. Nonferrous Met. Soc. China 23(2013) 3428−3433
Transactions of Nonferrous Metals Society of China
www.tnmsc.cn

Coal-based reduction mechanism of low-grade laterite ore

Yan-jun LI, Yong-sheng SUN, Yue-xin HAN, Peng GAO

College of Resources and Civil Engineering, Northeastern University, Shenyang 110819, China

Received 29 July 2013; accepted 30 September 2013

Abstract: A low-grade nickel laterite ore was reduced at different reduction temperatures. The morphology of metallic particles was investigated by scanning electron microscopy (SEM) and energy dispersive spectroscopy (EDS). Experimental results indicate that the metallic nickel and iron gradually assemble and grow into larger spherical particles with increasing temperature and prolonging time. After reduction, the nickel laterite ore obviously changes into two parts of Fe−Ni metallic particles and slag matrix. An obvious relationship is found between the reduction of iron magnesium olivine and its crystal chemical properties. The nickel and iron oxides are reduced to metallic by reductant, and the lattice of olivine is destroyed. The entire reduction process is comprised of oxide reduction and metallic phase growth.

Key words: nickel laterite ore; coal-based reduction; reduction mechanism; Fe−Ni metallic phase

1 Introduction

Nickel is an important metal used in the production of stainless steel and alloys [1]. Approximately 65% and 12% of the overall nickel consumption worldwide are primarily consumed in stainless steel production and in super alloy or nonferrous alloy manufacturing, respectively [2]. Nickel laterite ores, which comprise 73% of the world's proven nickel reserves (approximately 160 million tons), are the dominant source of nickel [3]. However, only 42% of the world's production of nickel comes from nickel laterite ores [4]. Nickel laterite ores are formed through long weathering of ultra-basic rocks containing iron and magnesium silicate minerals [5]. During weathering, nickel steeps out on the top layer deposit on the substratum. As a result, Mg^{2+} and Fe^{2+} in the lattice of corresponding silicates and ferric iron oxides are substituted by Ni^{2+}. In laterite ores, nickel is closely associated with iron oxide and silicate minerals. It serves as an isomorphous substitute for iron and magnesium in the lattice. Nickel laterite ores are difficult to beneficiate by physical methods because of their complex mineralogy [6]. Thus, metallurgical technology is usually applied to extracting nickel from nickel laterite ores.

In recent years, the rapid rise in stainless steel demand has dramatically increased the production of nickel metal by approximately 4.7% per year. Therefore, the recovery of nickel from laterite ores using pyrometallurgy has been extensively investigated. MICHAIL et al [7] investigated the microwave reduction of nickeliferous laterite ores. PURWANTO et al [8] recovered nickel and cobalt metals using selective reduction of laterite ores followed by acid leaching. LI et al [9] used reduction roasting followed by wet magnetic separation to beneficiate nickel and iron from nickeliferous laterites and investigated the effects of sodium sulfate. ZHU et al [10] upgraded low-nickel content laterite ores using selective reduction followed by magnetic separation. These previous studies demonstrated that coal-based reduction followed by magnetic separation is effective for the recovery of nickel and iron from nickel laterite ores. Ferronickel materials obtained from magnetic separation are directly used to manufacture stainless steels. During this process, the growth of metallic particles is critical because the particles must grow to a size large enough for subsequent magnetic separation [11,12]. However, most of these studies focused on the conditions during reduction and magnetic separation. The reduction mechanisms, especially the growth of metallic particles which is essential in separating Fe−Ni metallic iron phase and in controlling the reduction process, have not yet been

Foundation item: Project (51134002) supported by the National Natural Science Foundation of China; Project (2012BAB14B02) supported by the Ministry of Science and Technology of China; Project (12120113086600) supported by Ministry of Land and Resources of China
Corresponding author: Yan-jun LI; Tel: +86-24-83688920; E-mail: liyanjun@mail.neu.edu.cn
DOI: 10.1016/S1003-6326(13)62884-8

discussed well. Therefore, it is necessary to investigate the mechanisms of coal-based reduction of nickel laterite ore.

In this study, the reduction of nickel from a low-grade nickel laterite ore was performed using coal-based reduction. The effects of reduction temperature and time on the growth of metallic particles were investigated. Moreover, the reduction mechanisms of nickel were analyzed based on the crystal structure properties of the nickel laterite ore and the reduction process. The present study aims to provide a basis for the utilization of nickel laterite ores.

2 Experimental

2.1 Materials

A low-grade laterite ore from Burma was selected as the nickel-bearing ore. The chemical composition of the laterite ore is given in Table 1. Figure 1 shows the X-ray diffraction pattern of laterite. It can be seen from Table 1 and Fig. 1 that iron magnesium olivine is the essential mineral in the nickel laterite sample. The molecular formula is $(Mg^{2+},Fe^{2+},Ni^{2+})_2SiO_4$, where Mg^{2+}, Fe^{2+}, and Ni^{2+} are of isomorphism. The selected reductant is Shenfu coal from Shaanxi Province, China. The proximate analysis of the coal is listed in Table 2. The coal is a good reductant because of its high fixed carbon and volatile matter, low ash, and relatively low harmful element (S, P) content. The ore and coal were ground to 100% passing screen aperture of 2.0 mm before the reduction to increase the contact between them.

Table 1 Chemical composition of nickel laterite ore (mass fraction, %)

TFe	Ni	Mn	Co	SiO_2
14.24	2.26	0.24	0.05	41.41
MgO	Al_2O_3	CaO	Cr_2O_3	Fe_2O_3
17.24	1.99	0.26	1.99	20.00

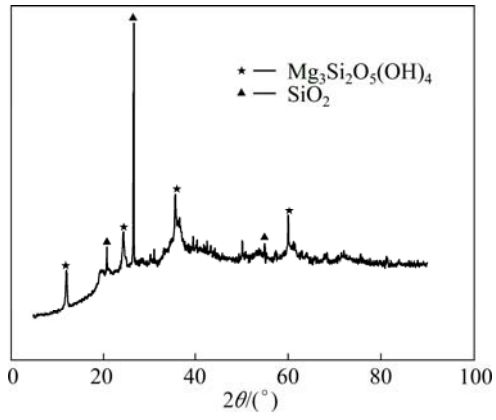

Fig. 1 XRD pattern of nickel laterite ore

Table 2 Proximate analysis of pulverized coal (mass fraction, %)

FC	VM	Ash	P	S	Al_2O_3	SiO_2	CaO
56.10	30.40	5.44	0.003	0.022	0.57	1.27	1.83

FC—Fixed carbon; VM—Volatile matter

2.2 Reduction experiment

The equipment for reduction was a SX-8-16 muffle furnace with a working chamber (200 mm× 200 mm × 150 mm). The heating rate of the furnace ranged from 10 °C/min to 20 °C/min, and the upper temperature limit was 1600 °C. Approximately 50 g of ore was used for each reduction experiment. The C/O ratio (i.e., the amount of coal addition in terms of gram-atomic ratio of the fixed carbon in the coal added to the combined oxygen in nickel and iron oxides) was 2.5. The dried mixture of ore and coal was placed in a ceramic crucible, which was then placed in a muffle furnace when the temperature of the furnace reached the reduction temperature. Once the reduction experiments were finished, the samples were taken out of the furnace and cooled to room temperature by water quenching. The reduced product was dried in a vacuum oven for SEM analysis.

2.3 Measuring method

To understand the changes in iron and nickel status during reduction, the microstructures of reduced materials of the nickel laterite ore under certain reduction conditions were investigated using SSX−550 SEM (SHIMADZU). The reduced product was ground to approximately less than 2.0 mm. To avoid the charging problem, gold film of a few nanometers was deposed on the reduced product powders placed on a conductive adhesive prior to SEM observation. Composition analysis was carried out by energy dispersive spectrometry (EDS) on an Inca X-ray spectrometer combined with an SEM.

3 Results and analysis

3.1 Effect of reduction temperature on growth of metallic particles

Reduction temperature is a key effective factor in metallic particle growth. The nickel laterite ore was reduced at various temperatures between 1200 and 1300 °C while keeping a reduction time of 40 min. The morphological features of the reduced material are shown in Fig. 2. The bright and white crystal points are Ni and Fe, which are the metal phases produced by reduction. The main grey points are Si, Mg, and Ca, which remain the original states before entering the furnace. SEM images show that metallic iron and nickel are melted and associated homogeneously in the form of

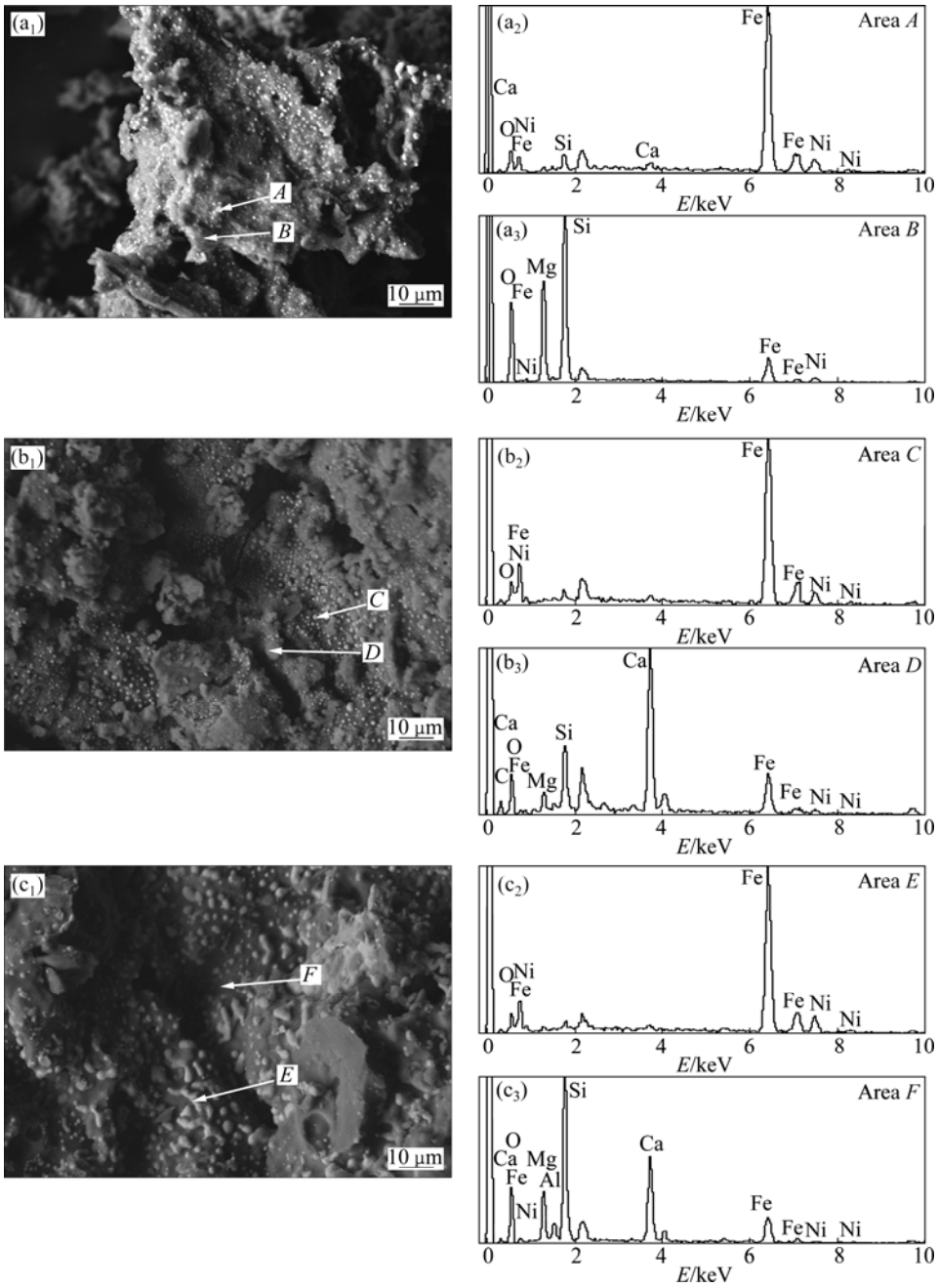

Fig. 2 SEM images and EDS patterns of reduction materials at different reduction temperatures: (a_1, a_2, a_3) 1200 °C; (b_1, b_2, b_3) 1250 °C; (c_1, c_2, c_3) 1300 °C

Fe−Ni metallic phase.

More nickel and iron particles are produced, and the particle size increases as temperature is increased from 1200 °C to 1300 °C. Meanwhile, the nickel and iron particles become increasingly spherical with increasing reduction temperature. More nickel and iron particles are chained at 1300 °C. The probable reason for this is that the fluidity of nickel and iron is better at high temperatures.

The increase in reduction temperature favors the cohesion between nickel and iron as well as the growth of metallic crystal particles. The purity of metallic particles increases. During metallic particle growth, metallic phases are produced firstly and then regenerated. As a result, the particles become purified gradually.

3.2 Effect of reduction time on growth of metallic particles

Tests at different reduction times were conducted to further realize the aggregation growth behaviors of metallic particles during the reduction process. Reduction temperature was fixed at 1275 °C. The morphological features of the reduced material are shown in Fig. 3. The SEM images and EDS analyses

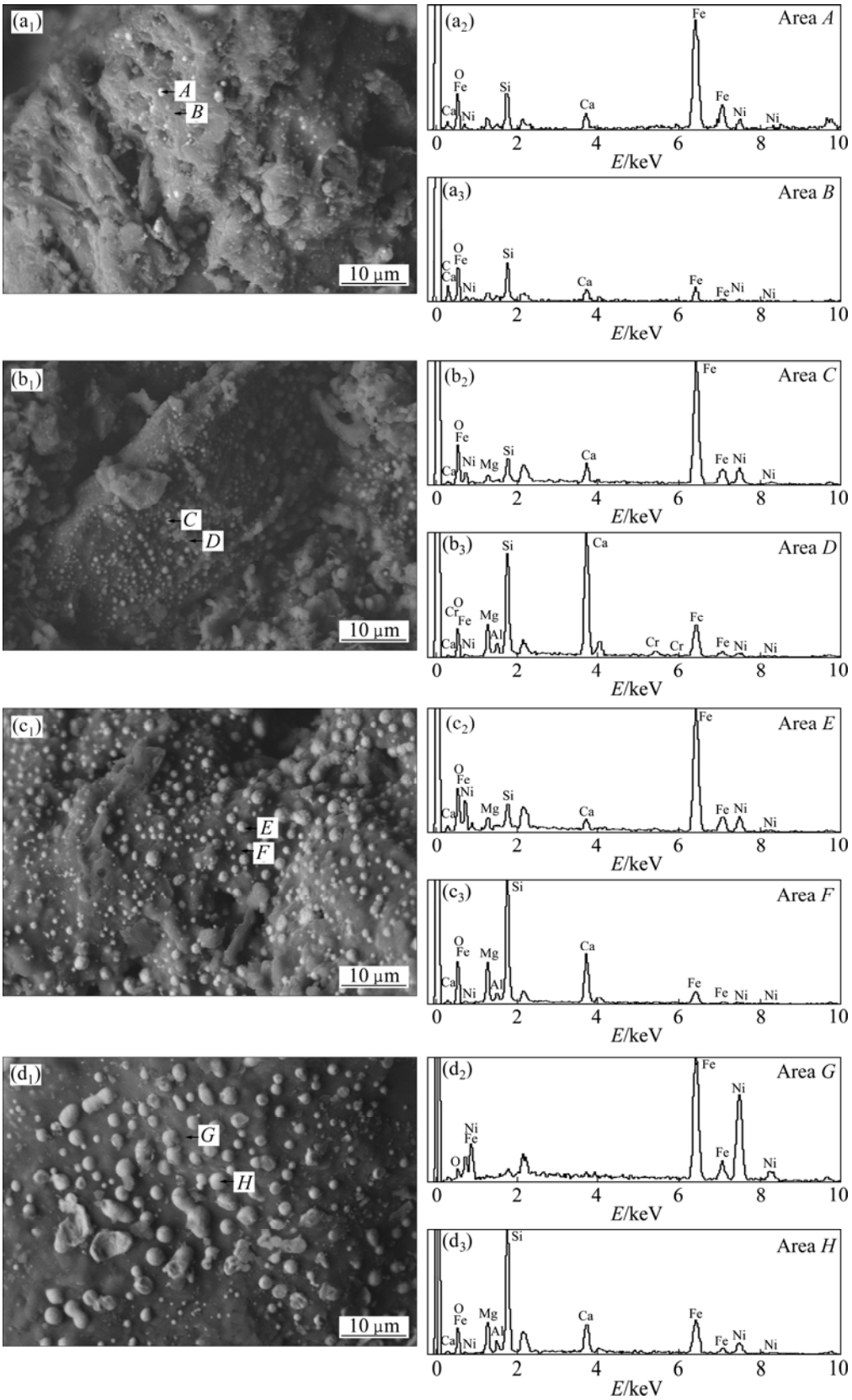

Fig. 3 SEM images and EDS patterns of reduction materials at different reduction times: (a_1, a_2, a_3) 20 min; (b_1, b_2, b_3) 40 min; (c_1, c_2, c_3) 60 min; (d_1, d_2, d_3) 80 min

indicate that the main elements of the bright and white crystal particles are Ni and Fe and that the basal corpuscle portion is mainly based on Si, Mg, and Ca. The metallic particles continuously grow as the reduction time in deep reduction is prolonged and the degree of sphericity is increased. Some nickel and iron particles

rupture when the reduction time is prolonged to 80 min. When the reduction time is prolonged to a critical value, the fluidity of nickalloy will increase, which causes the rupture of spherical particles.

The EDS patterns of the spots show that the peak values of the impurity elements of Si, Ca, and Al on the metallic surface continuously decrease as the reduction time is prolonged. Particularly, the peak value of nickel increases more significantly. This indicates that the purity of metallic particles increases as the reduction time is prolonged.

Comprehensive analyses show that the crystal grain size, sphericity degree, nickalloy particle impurity, nickel and iron liberation, and nickel matrix increase as the reduction time is prolonged. These results are beneficial for the magnetic separation of nickel and iron. However, over prolonged reduction time weakens the reduction atmosphere and oxidizes the metallic particles in the reduced material.

3.3 Reduction process

3.3.1 Crystal chemistry of nickel-containing minerals

The main chemical bonds in silicate minerals are ionic and covalent bonds. As the formation of ionic bonds among atoms in the mineral structure is increased, the polarity of bond increases, and the bond fractures easily. By contrast, as the formation of covalent bonds is increased, the degree of nonpolarity increases, and the bond fractures difficultly.

According to the Pauling's rules, λ is the ratio of bond power, and expresses the polarity of bond. In iron olive palygorskite, the λ values of Fe—O and Si—O are 0.94 and 0.63, respectively. In magnesia olivine palygorskite, the λ values of Mg—O and Si—O are 0.93 and 0.63, respectively. Hence, when iron magnesium olivine suffered from exogenic action, the prior fractured bond should be Fe—O and Mg—O. The Ni—O of iron magnesium olivine also belongs to the prior fractured bond [13,14].

The crystal chemical properties of nickel laterite ore show that Ni—O, Fe—O, and Mg—O fracture prior to Si—O. Therefore, Ni^{2+} and Fe^{2+} are reduced to metallic phase existing in the pore of the lattice prior to Mg^{2+} during reduction. Si exists in the slag phase because Si—O does not break.

3.3.2 Thermodynamic basis for nickel reduction

The reduction reactions of nickel oxide by solid carbon are shown as follows:

$$NiO+C=Ni+CO \quad (1)$$

$$2NiO+C=2Ni+CO_2 \quad (2)$$

The relative proportion of the products CO and CO_2 depends on system balance. According to the Boudouard reaction and the relationship between the equilibrium concentration of CO and the temperature under the standard atmospheric pressure, both CO and CO_2 are present in the equilibrium composition of carbonic gasification reaction when the reduction temperature is below 1000 °C. Thus, the reactions (1) and (2) occur simultaneously, indicating that NiO reacts with C to form Ni, CO, and CO_2. However, at higher temperatures (>1000 °C), CO_2 mostly transforms into CO in the C−CO−CO_2 system. Hence, in the present study, reaction (2) basically does not exist. The main reactions of nickel oxide to metallic nickel are shown as follows:

$$NiO+CO=Ni+CO_2 \quad (3)$$

$$CO_2+C=2CO \quad (4)$$

$$NiO+C=Ni+CO \quad (5)$$

The standard formation free energies (ΔG^{Θ}) of carbon oxide and nickel oxide are shown in Fig. 4. It can be seen that 725 K is the lowest temperature for NiO reduction by fixed carbon under the standard atmospheric pressure. In addition, the ΔG^{Θ} line of CO_2 generated by oxidized CO is always below the ΔG^{Θ} line of NiO, and the ΔG^{Θ} value of reaction (3) is negative at the standard atmospheric pressure. This indicates that NiO is easily reduced by CO.

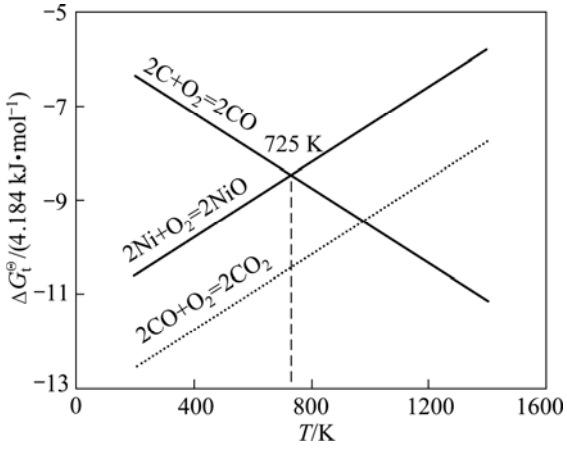

Fig. 4 Standard Gibbs free energies of carbon oxides and nickel oxide

3.3.3 Reduction mechanism analysis

In the selected ore sample, nickel exists in iron magnesium olivine as an isomorphous substitute for iron and magnesium in the lattice. Thus, the reduction of nickel consists of complex compound dissociation and simple oxide reduction, which makes the reduction of nickel laterite ore difficult. In the reduction, nickel is almost reduced by CO. Ni^{2+} and Fe^{2+} are reduced to metallic iron and nickel, and Ni—O and Fe—O bonds fracture, which destroy the lattice of olivine. The produced metallic iron and nickel existing in the pore of lattice have a lower melting point because of

carburization. Thus, they are energetically active and assemble to form superfine Fe−Ni metallic particles. As reduction time is prolonged, a large amounts of metallic iron and nickel atoms are produced. According to the principle of the minimum free energy, Ni and Fe diffuse to the superfine Fe−Ni metallic particles, whereas Fe−Ni metallic particles reunite and grow [15−17].

4 Conclusions

1) Reduction temperature and reduction time significantly influence the growth behavior of Fe−Ni metallic particles. The size and purity of the particles increase with increasing reaction temperature and prolonging reaction time. The Fe−Ni metallic phase is set in the matrix as spherical particles. The complicated particles of nickel laterite ore are changed into metallic particles and slag matrix after the reduction. The boundaries between metallic particles and slag matrix are clear; thus, the liberation of metallic particles can be easily achieved.

2) During the reduction, nickel is almost reduced by CO rather than C. An important relationship is found between the reduction process and the crystal structure and crystal chemical properties of the nickel laterite ore. The reduction comprises complex compound dissociation and simple oxide reduction. The reduction process damages the lattice of iron magnesium olivine. The reduced metallic iron and nickel gradually assemble and form larger metallic particles.

References

[1] CHANG Y F, ZHAI X J, FU Y. Phase transformation in reductive roasting of laterite ore with microwave heating [J]. Transactions of Nonferrous Metals Society of China, 2008, 18: 969−973.

[2] JOHNSON J, RECK B K, WANG T, GRAEDEL T E. The energy benefit of stainless steel recycling [J]. Energy Policy, 2008, 36(1): 181−192.

[3] LI B, WANG H, WEI Y G. The reduction of nickel from low-grade nickel laterite ore using a solid-state deoxidisation method [J]. Minerals Engineering, 2011, 24: 1556−1562.

[4] NORGATE T, JAHANSHAHI S. Assessing the energy and greenhouse gas footprints of nickel laterite processing [J]. Minerals Engineering, 2011, 24: 698−707.

[5] LANDERS M, GRFE M, GILKES R, SAUNDERS M, WELLS M. Nickel distribution and speciation in rapidly dehydroxylated goethite in oxide-type lateritic nickel ores: XAS and TEM spectroscopic (EELS and EFTEM) investigation [J]. Australian Journal of Earth Sciences, 2011, 58(7): 745−765.

[6] DALVI A D, BACON W G, OSBORNE R. The past and the future of nickel laterites [C]//PDAC 2004 International Convention. North Carolina, USA: Trade Show & Investors Exchange, 2004: 1−27.

[7] MICHAIL S, MARIA T, RON H, et al. Microwave reduction of a nickeliferous laterite ore [J]. Minerals Engineering, 2012, 34: 19−29.

[8] PURWANTO H, SHIMADA T, TAKAHASHI R, YAGI J I. Recovery of nickel from selectively reduced laterite ore by sulphuric acid leaching [J]. ISIJ International, 2003, 43(2): 181−186.

[9] LI G H, SHI T M, RAO M J, JIAN T, ZHANG Y B. Beneficiation of nickeliferous laterite by reduction roasting in the presence of sodium sulfate [J]. Minerals Engineering, 2012, 32: 19−26.

[10] ZHU D Q, CUI Y, VINING K, HAPUGODA S, DOUGLAS J, PAN J, ZHENG G L. Upgrading low nickel content laterite ores using selective reduction followed by magnetic separation [J]. International Journal of Mineral Processing, 2012, 106−109: 1−7.

[11] KO Y D, SHANG H. A neural network-based soft sensor for particle size distribution using image analysis [J]. Powder Technology, 2011, 212(2): 359−366.

[12] OTSUKI A, DODBIBA G, FUJITA T. Measurements of size distribution of titanium dioxide fine particles in a highly concentrated non-aqueous suspension by using particle self-assembly under an electric field [J]. Advanced Powder Technology, 2012, 23(4): 517−522.

[13] SUN Chuan-yao, YIN Wan-zhong. Floth flotation principle of silicate minerals [M]. Beijing: Science Press, 2001: 28−38. (in Chinese)

[14] SHAO Mei-chen. Pauling rules and bond-valence theory [M]. Beijing: Higher Education Press, 1993: 18−37. (in Chinese)

[15] SUN Y S, GAO P, HAN Y X, REN D Z. Reaction behavior of iron minerals and metallic iron particles growth in coal-based reduction of an oolitic iron ore [J]. Industrial & Engineering Chemistry Research, 2013, 52(6): 2323−2329.

[16] GAO P, SUN Y S, REN D Z, HAN Y X. Growth of metallic iron particles during coal-based reduction of a rare earths-bearing iron ore [J]. Minerals & Metallurgical Processing, 2013, 30(1): 74−78.

[17] XU C Y, SUN T C, KOU J, LI Y L, MO X L, TANG L G. Mechanism of phosphorus removal in beneficiation of high phosphorous oolitic hematite by direct reduction roasting with dephosphorization agent [J]. Transactions of Nonferrous Metals Society of China, 2012, 22: 2806−2812.

低品位红土镍矿深度还原机理

李艳军，孙永升，韩跃新，高 鹏

东北大学 资源与土木工程学院，沈阳 110819

摘 要：采用扫描电子显微镜和 EDS 能谱研究低品位红土镍矿深度还原过程中金属颗粒的生长行为，并在此基础上分析其还原机理。结果表明，金属铁和镍逐渐聚集生长为 Fe−Ni 颗粒，并且颗粒粒度随着还原温度的升高和还原时间的延长而明显增大。还原后，红土镍矿明显变为 Fe−Ni 金属颗粒和渣相基体两部分。铁镁橄榄石的还原与其晶体化学特性密切相关。铁和镍的氧化物被还原剂还原为金属铁和镍，同时，橄榄石的晶格结构被破坏。红土镍矿深度还原包含金属氧化物还原和金属相生长两个过程。

关键词：红土镍矿；深度还原；还原机理；Fe−Ni 金属相

(Edited by Xiang-qun LI)